IL NUOVO CIMENTO **44 C** (2021) 47
DOI 10.1393/ncc/i2021-21047-0

COMMUNICATIONS: SIF Congress 2020

Lifetime measurements of the 2_1^+, 4_1^+ and 6_1^+ states in ^{114}Pd

E. R. GAMBA(1)(2)(3)(*), G. BENZONI(2), A. M. BRUCE(3), S. LALKOVSKI(4)(5), M. RUDIGIER(4), S. BOTTONI(6), M. P. CARPENTER(6), S. ZHU(6)
and the FATIMA-GAMMASPHERE COLLABORATION

(1) *Museo Storico della Fisica e Centro Studi e Ricerche Enrico Fermi - Roma, Italy*
(2) *INFN, Sezione di Milano - Milano, Italy*
(3) *School of Computing, Engineering and Mathematics, University of Brighton Brighton, UK*
(4) *Department of Physics, University of Surrey - Guildford, UK*
(5) *Department of Nuclear Engineering, Faculty of Physics, University of Sofia St. Kl. Ohridski, Sofia, Bulgaria*
(6) *Physics Division, Argonne National Laboratory - Illinois, Argonne, USA*

received 14 January 2021

Summary. — Among the most important physical observables in nuclear structure are the lifetimes of nuclear excited states. Nuclei of ^{114}Pd, predicted by spectroscopic signatures to be candidates for γ-rigid triaxiality, were populated in the spontaneous fission of ^{252}Cf and the lifetimes of the 2_1^+, 4_1^+ and 6_1^+ states were measured via the fast-timing technique. The obtained lifetimes of $\tau_{2^+} = 103(10)$ ps, $\tau_{4^+} = 21(11)$ ps, and $\tau_{6^+} \leq 10$ ps, and the corresponding deduced $B(E2; I \rightarrow I\text{-}2)$ transition probabilities, indicate these to be collective states and also suggest the triaxial shape of ^{114}Pd to be more γ-rigid than its even-even neighbours in the $Z = 46$ isotopic chain.

1. – Introduction

The lifetime measurements of nuclear excited states serve as stringent tests for the predictions provided by theoretical models. Their importance as physical observables is in particular related to the occurrence of deformation across the nuclear chart. Quadrupole deformation parameters β_2 and γ can be deduced from $B(E2; I \rightarrow I\text{-}2)$ transition probabilities which, in turn, can be determined from the measured nuclear lifetimes. Among possible non-spherical shapes are oblate ($\beta_2 \leq 0$, $\gamma = \frac{n\pi}{3}$), prolate ($\beta_2 \geq 0$, $\gamma = \frac{n\pi}{3}$) and triaxial ($\gamma \neq \frac{n\pi}{3}$). The latter represents the case where all three nuclear axes take different lengths and the third axis length can be static (γ-rigid) or dynamical (γ-soft). The distinction between these different types of deformation can be made by using spectroscopic signatures and either intra- or inter-band $B(E2; I \rightarrow I\text{-}2)$ reduced transition probabilities. The $R_{4/2} = E_{4_1^+}/E_{2_1^+}$ ratio is a good signature for nuclear deformation and evolves from values of approximately 2 for nuclei close to shell closures, to the rigid

(*) E-mail: eugenio.gamba@mi.infn.it

rotor limit of 10/3. A $R_{4/2}$ that does not reach this rotational limit can indicate either transitional or triaxial nuclei. In particular, in the $A \simeq 110$ region of the nuclear chart of interest for this work, in the ruthenium ($Z = 44$) isotopic chain this ratio is always less than 10/3, suggesting either γ-soft or γ-rigid triaxial behaviour when far from shell closure. On the contrary nuclei belonging to the cadmium ($Z = 48$) isotopic chain are usually treated as vibrational, while palladium nuclei ($Z = 46$) lie somewhere in the middle of these two. The maximum value of the $R_{4/2}$ ratio, of approximately 2.6, is reached for $N = 68$ (^{114}Pd), expected to be the most deformed of this isotopic chain.

A common indicator of triaxiality is the energy of the 2_2^+ state relative to the energy of the 4_1^+ state. The ratio between the energy of these two states is expected to be around 1 or less for triaxial nuclei. This value is equal to 0.8 for ^{114}Pd . In order to distinguish between γ-rigid and γ-soft triaxiality, the *staggering parameter* $S(I)$ is often used [1]. For γ-rigid nuclei, $S(I)$ is expected to take negative values for the odd-spin levels and positive values for the even-spin ones, while the opposite is true for the γ-soft case. Using this criterion, an inversion of the type of triaxiality, from γ-soft to γ-rigid, can therefore be predicted for ^{114}Pd.

A more stringent test than the one provided by the staggering parameter can be obtained from $B(E2)$ measurements, for transitions between levels inside the ground-state band or in between the quasi-γ band and the ground-state band. In this work the $B(E2)$ measurements obtained for the $2_1^+ \rightarrow 0_{g.s.}^+$, $4_1^+ \rightarrow 2_1^+$ and $6_1^+ \rightarrow 4_1^+$ transitions in ^{114}Pd are presented.

2. – Experimental setup

A 34.4 μCi source of 183 ng of ^{252}Cf was placed at the focus of an hybrid 4π array made of two hemispheres of 51 Compton-suppressed high-purity germanium (HPGe) detectors from the Gammasphere array [2] and 25 $LaBr_3$:Ce fast scintillators from the FATIMA array [3]. In order to stop fission fragments from escaping either side of the disk-shaped source, the source was sandwiched between two platinum disks and neither Doppler-shifted γ rays nor increased line widths were observed. The 25 $LaBr_3$:Ce detectors consisted of 3.8 cm($\varnothing$) $\times$ 5.1 cm cylindrical crystals, coupled to a Hammamatsu H10570 photomultiplier assembly comprising a R9779 phototube. A 5 mm lead layer was employed to cover the side of each crystal in order to absorb Compton-scattered γ rays from adjacent crystals and to avoid cross-talk events. For the first time, a fully digital acquisition (DAQ) system was used for this scintillator array [3, 4]. Two different data streams were read out in parallel: on the $LaBr_3$:Ce side, fold $\geq$ 2 events made of γ rays within a time window of 200 ns were collected and, on the HPGe side, fold $\geq$1 events were stored independently. In a second stage, in order to obtain events of the type γ($LaBr_3$:Ce)-γ($LaBr_3$:Ce)-γ(HPGe), the two data streams were merged using a coincidence time window of 500 ns.

3. – Data analysis and results

The first step of the data analysis consisted in isolating the nucleus and excited levels of interest thanks to energy gates on the HPGe detectors, well known to be characterised by good energy resolution. For instance, in order to perform the lifetime measurement of the 2_1^+ level in ^{114}Pd, HPGe Full-Energy-Peak (FEP) gates were applied on the $6_1^+ \rightarrow 4_1^+$ (648 keV), $8_1^+ \rightarrow 6_1^+$ (715 keV), $10_1^+ \rightarrow 8_1^+$ (644 keV) and $5_1^- \rightarrow 4_1^+$ (1332 keV) transitions. A background energy gate was also identified for each one of these FEP gates. On the left-hand side of fig. 1, two HPGe and $LaBr_3$:Ce energy spectra are shown. These

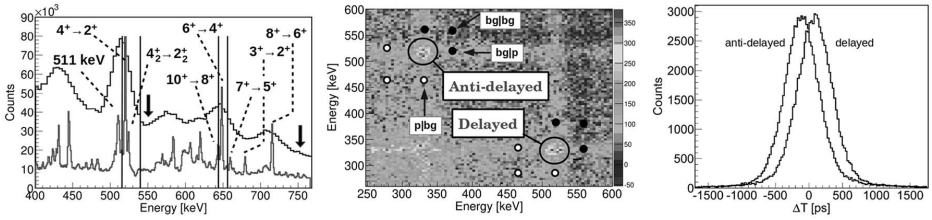

Fig. 1. – (Left) $LaBr_3$:Ce (dark grey, wide peaks) and HPGe (light grey, narrow peaks) energy spectra obtained from the procedure described in the text. (Centre) Two-dimensional projection of the start-stop cube obtained with the same procedure as for (left). The delayed and anti-delayed coincidence peaks as well as the three background regions are labelled. (Right) Delayed and anti-delayed time distributions, obtained by gating on the two coincidence peaks in (centre). Adapted from ref. [9].

were obtained by adding together the spectra produced by gating on each of the transitions listed above, and subtracting the four corresponding background contributions. These same FEP and background gates were then applied to the data set to make eight $\gamma(LaBr_3{:}Ce)$(start)-$\gamma(LaBr_3{:}Ce)$(stop)-ΔT cubes, where the time difference between the two coincident γ rays is given by $\Delta T = T_{stop} - T_{start}$. This set of eight cubes was then used to obtain the final $\gamma(LaBr_3{:}Ce)$(start)-$\gamma(LaBr_3{:}Ce)$(stop)-ΔT cube by adding together the four FEP-gated cubes and subtracting the four background-gated ones. A condition was applied so that no event was included more than once in this set of gates. The two-dimensional projection of the final start-stop cube is shown in the middle of fig. 1. The two coincidence peaks encircled by the black solid lines contain independent events from the $4_1^+ \rightarrow 2_1^+ \rightarrow 0_{g.s.}$ cascade. Given the definition of ΔT, if T_{start} is given by the time signal associated with the transition feeding the level of interest (and T_{stop} with the transition depopulating the same level), the delayed time distribution is obtained. If the opposite gates are applied the anti-delayed time distribution is produced instead. By gating on the two coincidence peaks, both delayed and anti-delayed distributions are obtained. The centroid difference between the delayed and anti-delayed time distributions can, in principle, provide a measure of the lifetime of interest (see the right-hand side of fig. 1), once the contribution of the time walk is taken into account by means of the prompt response difference curve (PRD), as described in ref. [5]. However, the contributions given by the high level of background shown in fig. 1 must be taken into account, as the time information carried by the γ-γ coincidences underneath the FEP-FEP coincidence peaks can modify the measured centroid positions. A careful evaluation of the contributions in the time information related to the background has been conducted as described in ref. [6].

From the background-corrected centroid difference value, it was then possible to perform the Generalised Centroid Difference Method [5], to measure the lifetime of the 2_1^+ state in ^{114}Pd to a value of $\tau = 113(5)$ ps. The weighted average of this value with the ones presented in refs. [7,8] gives $\tau_{2_1^+} = 103(10)$ ps.

An identical procedure, where different gates on both HPGe and $LaBr_3$:Ce energy information were considered, was performed for the lifetime measurements of the 4_1^+ and 6_1^+ states in ^{114}Pd and the values $\tau_{4^+} = 21(11)$ ps and $\tau_{6^+} \leq 10$ ps. were obtained [9].

4. – Interpretation of results

$B(E2; I \rightarrow I\text{-}2)$ transition probabilities were obtained from the measured lifetimes using the approach presented in ref. [10]. Values of 53(2) W.u., 43(27) W.u. and a lower limit of $\geq$21 W.u. were obtained for the $2_1^+ \rightarrow 0_{g.s.}^+$, $4_1^+ \rightarrow 2_1^+$ and $6_1^+ \rightarrow 4_1^+$ transitions,

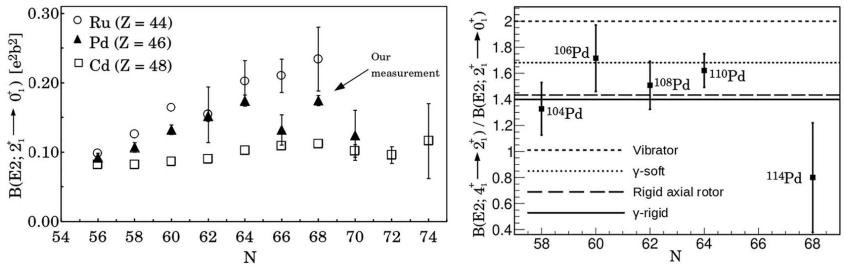

Fig. 2. – (Left) Experimental $B(E2; 2_1^+ \to 0_{g.s.}^+)$ values measured for the Ru, Pd and Cd isotopic chains. (Right) Available $R_{B(E2)}$ ratios for the Pd isotopic chain. The horizontal lines indicate the predictions of the vibrational, rotational, γ-rigid and γ-soft theoretical models. Adapted from ref. [9].

respectively. These values indicate the collective nature of the 2_1^+, 4_1^+ and 6_1^+ excited states. The comparison between the measured Ru, Pd and Cd $B(E2; 2_1^+ \to 0_{g.s.}^+)$ values are presented in fig. 2(left) in the range $N = 56$–72. An approximately constant value is observed for even-even Cd isotopes, usually treated as spherical harmonic vibrators. As the number of neutrons N increases, the Ru data follows a completely different path increasing up to a maximum value for ^{112}Ru, where the maximum of triaxiality is expected to occur [11]. The maximum value for the Pd isotopes is the one measured for ^{114}Pd at $N = 68$, suggesting that this nucleus is one of the most deformed ones of its isotopic chain.

The ratio $R_{B(E2)} = B(E2; 4_1^+ \to 2_1^+)/B(E2; 2_1^+ \to 0_{g.s.}^+)$ is also indicative of the degree of collectivity: $R_{B(E2)} = 2$ for vibrational nuclei, 1.43 for rigid axial nuclei, 1.68 for γ-soft rotors, and 1.40 for rigid triaxial rotors, in the case of $\gamma = 27.5°$. As shown in fig. 2(right) for $N \leq 64$, $R_{B(E2)}$ ratios for ^{104,106,108,110}Pd isotopes, obtained from Coulomb excitation, oscillate around the value predicted by the γ-soft model, in agreement with the prediction of the staggering parameter $S(I)$. Despite the large experimental uncertainty, for ^{114}Pd, the $R_{B(E2)}$ ratio takes the value of 0.80(42). This represents a sudden drop with respect to ^{104,106,108,110}Pd, and it is consistent within 1.4σ of the value predicted by the rigid triaxial rotor model, and also in agreement with the prediction of an inversion of the type of triaxiality at $N = 68$.

* * *

This work was financially supported by the STFC Grants No. ST/L005840/1, No. ST/L005743/1, and No. ST/G000751/1. It has also been partially supported by the U.S. Department of Energy, Office of Science, Office of Nuclear Physics under Contract No. DE-AC02-06CH11357 (ANL). This research used resources of the Argonne National Laboratory ATLAS facility, which is a DOE Office of Science User Facility.

REFERENCES

[1] Frauendorf S., *Int. J. Mod. Phys.*, **48** (2015) 1541001.
[2] Lee I.-Y. *et al.*, *Nucl. Instrum. Methods Phys. Res. Sect. A*, **520** (1990) c641.
[3] Rudigier M. *et al.*, *Nucl. Instrum. Methods Phys. Res. Sect. A*, **969** (2020) 163967.
[4] Rudigier M. *et al.*, *Acta Phys. Pol. B*, **48** (2017) 351.
[5] Régis J.-M. *et al.*, *Nucl. Instrum. Methods Phys. Res. Sect. A*, **191** (2013) 726.
[6] Gamba E. R. *et al.*., *Nucl. Instrum. Methods Phys. Res. Sect. A*, **928** (2019) 93.
[7] Dewald A. *et al.*, *Phys. Rev. C*, **78** (2008) 051302(R).
[8] Mach H. *et al.*, *JYFL Annual Report* (2003).
[9] Gamba E. R. *et al.*, *Phys. Rev. C*, **100** (2019) 044309.
[10] Raman S., Nestor C. J. and Tikkanen P., *At. Data Nucl. Data Tables*, **78** (2001) 1.
[11] Doherty D. T. *et al.*, *Phys. Lett. B*, **766** (2017) 334.